Negative differential thermal resistance in one-dimensional hard-point gas models

Rongxiang Luo

Department of Physics, Key Laboratory of Low Dimensional Condensed Matter Physics (Department of Education of Fujian Province), and Jiujiang Research Institute, Xiamen University, Xiamen 361005, Fujian, China

(Received 8 November 2018; published 28 March 2019)

We study negative differential thermal resistance (NDTR) of one-dimensional hard-point gas models. The models are non-integrable unless all particles have the same mass. We show that NDTR can exist in both the integrable case and the non-integrable case. In the integrable case, the existence of NDTR is analytically predicted and numerically confirmed and a mechanism for NDTR different from that observed in lattice models is unveiled. In the non-integrable case, we show that the mechanism also works under certain conditions and the properties of NDTR are found to depend on the particle masses and the system size by the molecular dynamics simulations. These results shed new light on the mechanisms for NDTR and may help design new functional heat devices.

DOI: 10.1103/PhysRevE.99.032138

I. INTRODUCTION

Due to the growing energy demand and the depletion and environmental impact of fossil fuels, renewable and environmentally friendly energy resources are always desired. In this framework, new functional heat devices [1] will play an important role and may be part of the dynamic mix in the future. A crucial point for the implementation of these heat devices is based on an indepth and comprehensive understanding of various heat transport phenomena [2], such as the thermoelectricity, thermal rectification, negative differential thermal resistance (NDTR), thermal cloaking, and so on. So far these heat transport phenomena have attracted intensive studies (see Refs. [1,2] for reviews and references therein). In the present paper, the heat transport problems associated with NDTR will be studied.

As is well known, the Fourier law describes how the heat current is sustained by the temperature gradient, i.e.,

$$J = -\kappa \nabla T, \tag{1}$$

where J is the heat current, κ is the heat conductivity, and ∇T is the temperature gradient. The Fourier law implies that in the linear response regime (∇T is sufficiently small), the heat current is proportional to the temperature gradient. However, an interesting and nontrivial phenomenon, i.e., the NDTR effect, may take place in a system where the heat current counterintuitively decreases as the temperature gradient increases.

In 2004, NDTR was first noticed by Li *et al.* in the study of asymmetric heat conduction [3], where it has been shown to be pivotal to design a thermal diode with an enormous rectification factor, and two years later the thermal transistor was shown to be possible because of NDTR [4]. Since then NDTR has attracted considerable interests for designing new functional heat devices based on the possibility to control the heat current. So far it has been shown in the theoretical models that NDTR plays a critical role in the design of various heat devices [4–7]. As few real systems have been chosen for investigating NDTR, the experimental progress for studying NDTR is relatively slow. However, a piece of good news is that in recent years, NDTR has been numerically shown to exist in the graphene nanoribbons [8–10] and the carbon nanotubes [11,12], which may provide new guidings to the NDTR experiment.

Theoretically, in the past decade, NDTR has been intensively studied in low-dimensional lattice models for identifying its mechanisms and related properties. So far NDTR has been found in various non-integrable lattices, such as the hybrid Frenkel-Kontorova (FK) lattices with weak links [4], the anharmonic lattice with gradient mass [13,14], the pure ϕ^4 [15] and FK models [16], the double-stranded systems [17], the two-segment Fermi-Pasta-Ulam lattice [18], etc. Meanwhile, the dependence of NDTR on different parameters such as the system size [19,20], temperature range [19], coupling strength [20–22], homogeneity [13,16], thermal dependence of conductivity [23], and the effect of on-site potential [4,5] have been considered. Moreover, in view of the phonon being responsible for the transmission of sound and heat, the phenomenon of NDTR can be understood from phonon-phonon interactions [4] and dynamical localization of phonon modes [24] in the presence of nonlinearity. It is worth to recall that by using analytical approaches the necessary ingredients for the occurrence of NDTR have already been reported [23,25].

Considering the significance of designing the solid-state thermal functional devices, the various lattice models do deserve to be intensively taken in the study of NDTR. In contrast, the gas models representing fluids have not been adopted to study NDTR yet. Actually, the gas models should not be neglected since the heat transport properties of the gas models are different in many respects from those of the lattice models, implying that the gas models could provide new perspectives for NDTR. For example, the heat carriers in the gas models may be the electrons that can be controlled by applying an electromagnetic field, but it is impossible to control the phonons in the same way. Therefore, in order to obtain more comprehensive understanding to NDTR and to help find new potential applications, it is worth

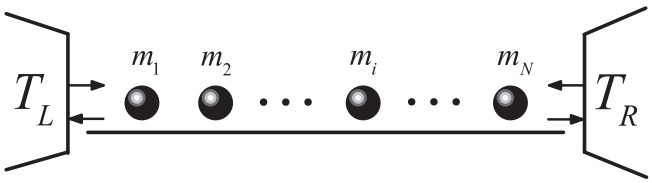

FIG. 1. Scheme of the 1D hard-point gas model studied in this paper. It consists of N hard-point, elastically colliding particles with mass m_i, and two heat baths with different temperature T_L and T_R. See text for more details.

to extend the study of NDTR to the gas models. Just like studying the lattice models, some similar questions can be raised for the gas models. For instance, does the NDTR effect exist in the gas models? If it exists, what is the underlying mechanism and related properties?

In this work we will attempt to answer these questions. For simplicity, we consider one-dimensional (1D) hard-point gas models as illustrating examples. Indeed, they are clean and simple billiard-type systems, which have been widely used to understand the general transport properties of classical dynamical systems. Moreover, an important feature of billiard-type systems is that their dynamical properties do not depend on the temperature, which makes their analysis even more simplified. By analyzing the hard-point gas models, we will show that they exhibit the NDTR effect in both the integrable and non-integrable cases. Importantly, a mechanism for NDTR observed in gas models will be revealed. In addition, our numerical results will show that in the non-integrable cases, the properties of NDTR depend on the particle masses and the system size.

The paper is organized as follows. The model and numerical details are introduced in Sec. II. Section III is devoted to analyze the mechanism and properties of NDTR in the integrable case. In Sec. IV, we show that the mechanism also works under certain conditions in the non-integrable cases and the related properties of NDTR are investigated by the molecular dynamics simulations. Finally, some related issues will be discussed with a brief summary in Sec. V.

II. 1D HARD-POINT GAS MODEL

Since 1965 when Jepsen proposed the 1D hard-point gas model [26], by using or transforming this model, researchers have obtained great achievements for understanding various aspects of 1D transport [27–33]. Here, it is taken as an illustrating example to show that NDTR can exist in the gas models. The model (see Fig. 1) consists of N hard-point, elastically colliding particles with mass m_i, $i = 1, \ldots, N$. Here, the length of the system is denoted as L, and we fix the averaged particle number density to be unity so that $N = L$. All particles move freely and independently except elastic collisions with their nearest neighbors. When two particles meet, the particles' velocities are updated by the following formula:

$$v_i' = \frac{m_i - m_j}{m_i + m_j} v_i + \frac{2m_j}{m_i + m_j} v_j,$$
$$v_j' = \frac{2m_i}{m_i + m_j} v_i - \frac{m_i - m_j}{m_i + m_j} v_j, \tag{2}$$

where j denotes $i + 1$ or $i - 1$. In order to compute the heat current of the system, we couple its two ends to two statistical heat baths at different temperature T_L (left) and T_R (right). When the first (last) particle hits the left (right) boundary of the system, it is reflected back with a new speed $|v|$ given by the probability distribution [34]

$$f_{L,R}(v) = \frac{|v| m_{1,N}}{k_B T_{L,R}} \exp\left(-\frac{v^2 m_{1,N}}{2 k_B T_{L,R}}\right), \tag{3}$$

where $v \geqslant 0$ for the left bath and $v \leqslant 0$ for the right bath, and k_B is the Boltzmann constant.

In our numerical simulations, the temperatures of the baths are set to be $T_L = T(1 + \Delta)$ and $T_R = T(1 - \Delta)$, where T is the nominal system temperature and Δ is the temperature bias. Before the evolution of the system, each particle is given initially a random coordinate and a random velocity according to the Boltzmann distribution at the temperature T. Then the system is evolved by using an effective event-driven algorithm [35]. After the system reaches the steady state, we compute the steady heat current J according to the heat current definition [27], i.e., the averaged energy exchanged in the unit time between a boundary particle and the heat bath. In addition, the distribution function of temperature $T(x)$ and particle density $\rho(x)$, where x is the space variable, are measured as well. For calculating $T(x)$ and $\rho(x)$, we divide the space of the system into the $N_a = \frac{L}{a}$ bins of equal size a. The total kinetic energy and the total number of particles observed in the ith bin in a unit time are denoted by $\mathcal{E}_i$ and $\mathcal{N}_i$, thus $T(ia)$ and $\rho(ia)$ are respectively defined as $T(ia) = \langle \mathcal{E}_i/a \rangle$ and $\rho(ia) = \langle \mathcal{N}_i/a \rangle$, where $\langle \cdot \rangle$ represents the time average. We emphasize that in our simulations, we set $T = k_B = a = 1$ throughout and long enough integration times ($>10^8$) so that the error bars for all the measured values of J are much smaller than the data symbols representing them.

III. THE PROPERTIES OF NDTR IN THE INTEGRABLE CASE

Here, we show that NDTR exists in the integrable 1D hard-point gas model and reveal its mechanism. If all particles have the same mass m, $m_i = m$, then the model is integrable and, considering the heat bath given by Eq. (3), the heat current J that crosses the system can be written as (see Appendix for the derivation)

$$J = \frac{N}{L} \sqrt{\frac{2k_B^3}{m\pi}} \sqrt{T_L T_R} (\sqrt{T_L} - \sqrt{T_R}). \tag{4}$$

By substituting $T_L = T(1 + \Delta)$ and $T_R = T(1 - \Delta)$, Eq. (4) can be rewritten as

$$J = \frac{N}{L} \sqrt{\frac{2k_B^3 T^3}{m\pi}} \sqrt{1 - \Delta^2} (\sqrt{1 + \Delta} - \sqrt{1 - \Delta}). \tag{5}$$

Note that the temperature difference ΔT, $\Delta T = T_L - T_R = 2T\Delta$, is a linear function of Δ. Based on Eq. (5), the heat current is equal to zero when $\Delta = 0$ or $\Delta = 1$ and the heat current maximum, $J_{\max}$, is reached at the critical value $\Delta_{cr} = \sqrt{5}/3$, which means that the heat current increases to the maximum and then decreases to zero with increasing Δ from

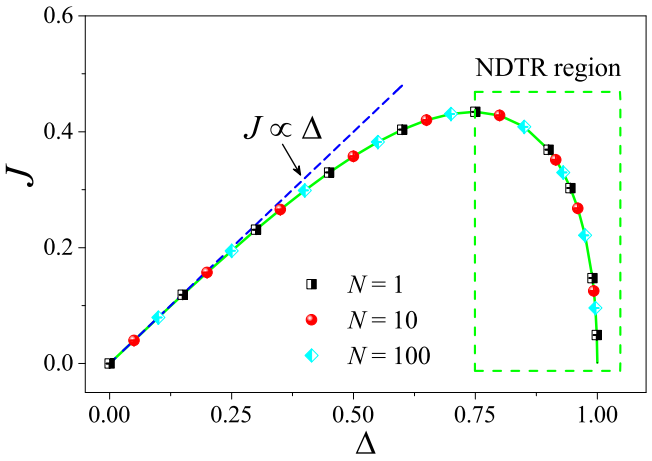

FIG. 2. The heat current as a function of Δ for the integrable case. The symbols are for the numerical results, and the companying green curve is the analytical result given by Eq. (5). For reference the blue-dashed line is the best linear fit, $J \propto \Delta$. Here, the particle mass is set to be unity.

zero to one. Based on the above analysis, we conclude that the system affirmatively exhibits the NDTR effect.

To confirm the above arguments, we turn to the help of numerical simulations. In Fig. 2, we show the heat current J as a function of Δ, where the symbols are obtained by the numerical simulations. It can be seen that for small Δ ($\Delta < 0.25$), the heat current J follows the linear response prediction by the Fourier law, but as Δ is increased further, the heat current J increases to the maximum and then decreases to zero in a way that is no longer linear, and the NDTR effect (the region with a green frame) is clearly seen. These numerical results are compared with the analytical result given by Eq. (5) and the agreement is perfect. Note that for the integrable case, the existence of NDTR does not depend on the particle number N, the temperature T, and the particle mass m as shown in Eq. (5).

Here, we would like to point out that for having NDTR, it does not suffice to increase the temperature gradient, but in doing so one has to lower temperature at either of the sides. If the temperatures of the baths are set to be T and $T(1+\Delta)$, it can be seen from Eq. (4) that the NDTR effect can be observed when keeping T fixed and lowering Δ. Moreover, one point that need to be stressed is that due to the dynamical properties of this system, the heat current follows the scaling relation $J(cT, c\Delta) = \sqrt{c^3}J(T, \Delta)$. Note that this scaling relation applies not only to the integrable case but also to the non-integrable case.

Why does the NDTR effect exist in the integrable gas model? To understand the mechanism, it is helpful to consider an extreme case that the system consists of only one particle and the temperature of the cold bath tends to zero, i.e., $T_R \to 0$. In this extreme case, the particle will be reflected back with a very slow speed ($v \to 0$) when it collides with the right boundary of the system, which could be imagined that this particle is frozen by the cold bath. As a result, there will be no heat current between the baths when $\Delta \to 1$ as shown in Fig. 2. Similarly, for more particles, the reason for zero current at $\Delta \to 1$ could be explained as follows: The first particle reaching the cold bath is stopped immediately; Then the next particle colliding with the first one is stopped after the collision, since when two particles with same mass collide they simply exchange their velocities; So all particles, by a chain of the collision events, are stopped one by one and no current remains. With decreasing the temperature of the cold bath, the motion of gas particles is restricted gradually by the cold bath, leading to the heat exchange between the baths is impeded. Note that this mechanism is different from that observed in the lattice models. This is because, unlike gas particles, the phonons that do not possess the mass are quasiparticles representing mechanical vibration, hence the heat current features of phonons are distinct from that of matter current. This may be the reason why the NDTR effect can be found in the integrable gas model but not in the integrable lattice model.

It is worth pointing out that the integrable case is special since there is no temperature gradient between the baths and the heat transport is ballistic. Now, the more important question is whether the mechanism is also applicable to the more general case where the system is non-integrable. This will be studied in the next section.

IV. THE PROPERTIES OF NDTR IN THE NON-INTEGRABLE CASES

In the nonlinear response regime, a rigorous analytical approach to study the properties of this non-integrable model has been so far unavailable. One usually has to rely on the molecular dynamics simulations. In the following, by using the method of simulation, we will show that the mechanism presented above may also work in the more general non-integrable cases where the heat transport is not ballistic. For illustrative purposes, the diatomic chain and the mass gradient chain are investigated, respectively.

A. The diatomic chain

If the particles shown in Fig. 1 are alternatively arranged with two different masses m and M (for odd- and even-numbered particles, respectively), we obtain a 1D diatomic chain. For convenience, we set $m \equiv 1$ so that M also refers to the mass ratio M/m. In the following, the dependence of heat current J on the temperature bias Δ is numerically studied for various mass ratio M.

The simulations results are shown in Fig. 3(a). It can be seen that the system does exhibit the NDTR effect, although the region of NDTR decreases and finally disappears with increasing M. In Fig. 3(b), we plot the temperature, particle density, and pressure profiles for different values Δ with $M = 1.2$. It can be seen that the pressure is uniform, which obeys the ideal gas law $P(x) = \rho(x)T(x)$. It can also be seen that the particle density at the right side of the system increases with increasing Δ, implying that when the temperature of the cold bath is colder, the more particles will be frozen by the cold bath. Moreover, we plot in Fig. 3(c) the collision rate that the boundary particle collides with the hot bath for different values Δ. It can be seen that for $M = 1.2$, the rate decreases with increasing Δ, as expected since the time that the boundary particle reflecting back to hot bath will be increased when the

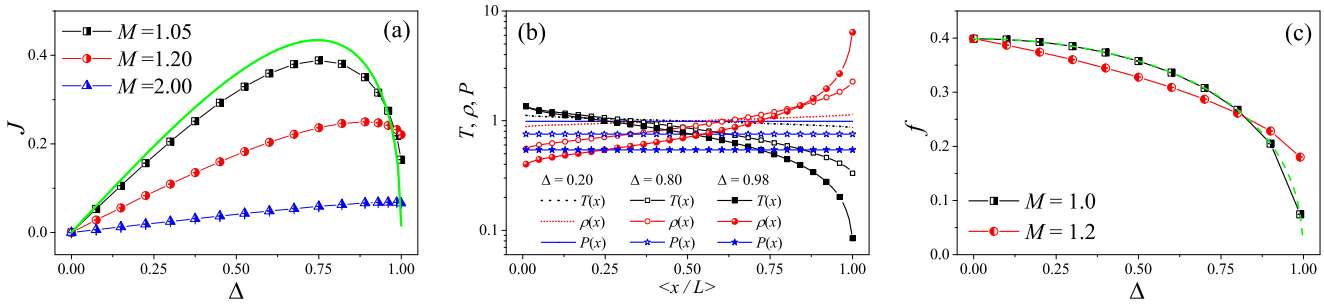

FIG. 3. (a) The heat current as a function of Δ for various mass ratio M. The green curve is the analytical result given by Eq. (5). (b) The temperature, particle density, and pressure profiles for different values Δ with $M = 1.2$. (c) The collision rate that the boundary particle collides with the hot bath as a function of Δ for integrable and non-integrable cases. The green dashed is the analytical result given by Eq. (6). Here, the data are obtained for $N = 101$.

cold bath is colder. This is a strong indication that the motion of gas particles is gradually restricted by the cold bath when lowering the temperature of the cold bath.

For the integrable case, the collision rate that the boundary particle collides with the bath can be written as (see Appendix for the derivation)

$$f = \frac{N}{L}\sqrt{\frac{2k_B}{m\pi}}\Big/\left(\frac{1}{\sqrt{T_L}} + \frac{1}{\sqrt{T_R}}\right). \tag{6}$$

In Fig. 3(c), this analytical expression is in good agreement with our numerical results. It shows that the collision rate decreases with decreasing T_R (or increasing Δ), which is the same as that for the non-integrable case. Based on the above analysis, we conclude that the mechanism for the NDTR effect is applicable to both the integrable and non-integrable cases.

Besides, we are curious about how the system size affects the NDTR effect when the mass ratio is fixed. In Fig. 4, we show the numerical results for various system size N when $M = 1.2$. It can be seen that the region of NDTR decreases and finally disappears when N is increased, suggesting that the properties of NDTR depend on the system size.

B. The mass gradient chain

Next, we consider the mass gradient chain, where the particle masses of the system form a gradient. In our simulations,

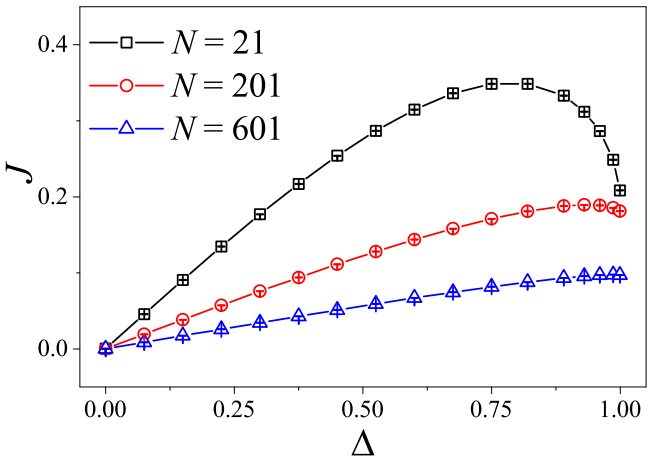

FIG. 4. The heat current as a function of Δ for various system size N. The mass ratio is $M = 1.2$.

the mass of ith particle is set to be $m_i = m_1 + (i-1)\xi$, where ξ is the mass gradient of the system and m_1 is set to be unity. Moreover, considering the system is asymmetric, we will exchange the temperatures of the baths, i.e., $\Delta \in [-1, 1]$ will be taken into account. Note that when $\Delta > 0$, the left end of the system is coupled to the hot bath, implying that the heat current is in the direction of increasing particle masses, and vice versa when $\Delta < 0$. In the following, we will focus on how the heat current J depends on the temperature bias Δ and on the mass gradient ξ.

The simulations results are shown in Fig. 5(a). As a reference, the result for the integrable case ($\xi = 0$) is plotted as well. Again, it can be seen clearly that the system presents the NDTR effect for both $\Delta > 0$ and $\Delta < 0$. In order to show that the mechanism also works here, the particle density profiles for different values Δ when $\xi = 0.1$ is plotted in Fig. 5(b). Our results suggest that no matter $\Delta > 0$ or $\Delta < 0$, the more particles will remain in the cold side when the temperature of the cold bath is decreased. This result is the same as that for the diatomic case.

In Fig. 5(a), it can also be seen that the properties of NDTR are different between $\Delta < 0$ and $\Delta > 0$. For $\Delta < 0$, the region of NDTR increases and always exists when ξ is increased. In contrast, for $\Delta > 0$, the region of NDTR decreases and finally disappears when ξ is increased. Note that the heat current is not equal to zero when $\Delta \to 1$, which is also different from that for the integrable case. The reason is that a light-mass particle can be reflected back to the hot bath when it collides with a heavy-mass particle, thus the heat energy transmission between the baths is not zero. However, the situation is different for $\Delta \to -1$ ($T_L \to 0$): The first particle reaching the cold bath is stopped immediately; Then the next particle colliding with the first one keeps a positive but smaller speed after the collision, the first one is stopped immediately after colliding with the heat bath, so the second one collides again and loses more speed and by a chain of these events in fact is stopped instantaneously as well; So all particles are stopped one by one and no current remains. Therefore, the different properties for NDTR between $\Delta < 0$ and $\Delta > 0$ are induced by the mass gradient.

Finally, for the mass gradient $\xi = 1$, the dependence of the NDTR effect on the system size is studied as well. The numerical results are shown in Fig. 5(c). For $\Delta < 0$, the region of NDTR increases and always exists when N is increased. In

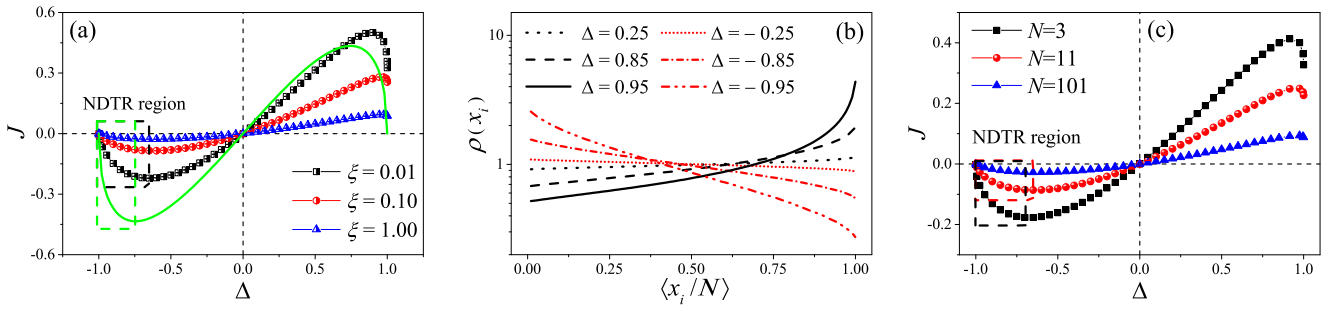

FIG. 5. (a) The heat current as a function of Δ for various mass gradient ξ. The symbols are for the numerical results, and the green curve is the analytical result given by Eq. (5). (b) The particle density profiles for different values Δ when $\xi = 0.1$. In (a) and (b), the system size is $N = 101$. (c) The heat current as a function of Δ for various system size N. In (c), the mass gradient is $\xi = 1$. Dashed lines are drawn for reference.

contrast, for $\Delta > 0$, the region of NDTR decreases and finally disappears when N is increased. The same property of NDTR for both $\Delta > 0$ and $\Delta < 0$ is that the smaller the system size, the more obvious the NDTR effect.

V. SUMMARY AND DISCUSSIONS

In conclusion, we have presented a mechanism for the NDTR effect that can work in both the integrable and non-integrable 1D hard-point gas models. This mechanism is fairly simple. It is based on the fact that with decreasing the temperature of the cold bath, the motion of the gas particles will be weakened gradually by the cold bath, thus leading to the heat exchange between the baths being impeded. Furthermore, our numerical results suggest that in the non-integrable cases, the region and existence of NDTR are found to depend on the particle masses and the system size. While we have considered for illustrative purposes a 1D hard-point gas models, we conjecture the same mechanism also works in other gas models, also of higher dimensions. This is mainly because the interactions between gas particles and heat baths are not limited by the spatial dimensions. Finally, we conjecture that the NDTR effect of the gas model might be observed and find applications in the context of cold atomic gases, where the thermoelectric effects have already been observed for weakly interacting particles [36].

APPENDIX: DERIVATION OF EQS. (4) AND (6)

First, let us consider the case that the system consists of one particle only. When the particle hits the left (right) boundary of the system, the average kinetic energy E_L (E_R) reflecting back to the system can be written as

$$E_{L,R} = \int_0^\infty \frac{1}{2} m v^2 f_{L,R}(v) dv = k_B T_{L,R}. \tag{A1}$$

The average time that a particle moves from the left boundary to the right boundary can be written as

$$t_{L\to R} = \int_0^\infty \frac{L}{v} f_L(v) dv = L\sqrt{\frac{m\pi}{2k_B T_L}}. \tag{A2}$$

Similarly, we can obtain $t_{R\to L}$ as well. The heat current, $J^{(1)}$, can thus be obtained according to the heat current definition $J^{(1)} = (E_L - E_R)/(t_{L\to R} + t_{R\to L})$, which reads as

$$J^{(1)} = \frac{1}{L}\sqrt{\frac{2k_B^3}{m\pi}}\sqrt{T_L T_R}(\sqrt{T_L} - \sqrt{T_R}). \tag{A3}$$

It can be seen from Eq. (2) that when two particles with same mass collide, they simply exchange their velocities. Thus, if the model consists of N particles with same mass, it is equivalent to a system with N noninteracting particles, the heat current can then be written as

$$J = NJ^{(1)} = \frac{N}{L}\sqrt{\frac{2k_B^3}{m\pi}}\sqrt{T_L T_R}(\sqrt{T_L} - \sqrt{T_R}). \tag{A4}$$

The collision rate that one particle collides with the bath is defined as $f^{(1)} = \frac{1}{t_{L\to R} + t_{R\to L}}$, thus if the model consists of N particles, the collision rate is

$$f = Nf^{(1)} = \frac{N}{L}\sqrt{\frac{2k_B}{m\pi}} \Big/ \left(\frac{1}{\sqrt{T_L}} + \frac{1}{\sqrt{T_R}}\right). \tag{A5}$$

[1] N. B. Li, J. Ren, L. Wang, G. Zhang, P. Hanggi, and B. Li, Rev. Mod. Phys. **84**, 1045 (2012).
[2] M. Maldovan, Nature **503**, 209 (2013).
[3] B. Li, L. Wang, and G. Casati, Phys. Rev. Lett. **93**, 184301 (2004).
[4] B. Li, L. Wang, and G. Casati, Appl. Phys. Lett. **88**, 143501 (2006).
[5] L. Wang and B. Li, Phys. Rev. Lett. **99**, 177208 (2007).
[6] L. Wang and B. Li, Phys. Rev. Lett. **101**, 267203 (2008).
[7] J. P. Wu, L. Wang, and B. Li, Phys. Rev. E **85**, 061112 (2012).
[8] J. N. Hu, Y. Wang, A. Vallabhaneni, X. L. Ruan, and Y. P. Chen, Appl. Phys. Lett. **99**, 113101 (2011).
[9] B. Q. Ai, W. R. Zhong, and B. Hu, J. Phys. Chem. C **116**, 13810 (2012).
[10] Z. G. Shao, B. Q. Ai, and W. R. Zhong, Appl. Phys. Lett. **104**, 013106 (2014).
[11] B. Q. Ai, M. An, and W. R. Zhong, J. Chem. Phys. **138**, 034708 (2013).

[12] Y. L. Ou, S. C. Lu, and B. Q. Ai, J. Stat. Mech. (2017) 053209.
[13] N. Yang, N. Li, L. Wang, and B. Li, Phys. Rev. B **76**, 020301(R) (2007).
[14] E. Pereira, Phys. Rev. E **82**, 040101(R) (2010).
[15] D. He, S. Buyukdagli, and B. Hu, Phys. Rev. B **80**, 104302 (2009).
[16] D. He, B. Q. Ai, H. K. Chan, and B. Hu, Phys. Rev. E **81**, 041131 (2010).
[17] W. R. Zhong, Phys. Rev. E **81**, 061131 (2010).
[18] W. R. Zhong, M. P. Zhang, B. Q. Ai, and B. Hu, Phys. Rev. E **84**, 031130 (2011).
[19] W.-R. Zhong, P. Yang, B.-Q. Ai, Z.-G. Shao, and B. Hu, Phys. Rev. E **79**, 050103(R) (2009).
[20] Z. G. Shao, L. Yang, H. K. Chan, and B. Hu, Phys. Rev. E **79**, 061119 (2009).
[21] D. Segal, Phys. Rev. B **73**, 205415 (2006).
[22] W. Chung Lo, L. Wang, and B. Li, J. Phys. Soc. Jpn. **77**, 054402 (2008).
[23] H. K. Chan, D. He, and B. Hu, Phys. Rev. E **89**, 052126 (2014).
[24] W. C. Fu, T. Jin, D. He, and S. X. Qu, Physica A **433**, 211 (2015).
[25] M. S. Mendonca and E. Pereira, Phys. Lett. A **379**, 1983 (2015).
[26] D. W. Jepsen, J. Math. Phys. **6**, 405 (1965).
[27] G. Casati, Found. Phys. **16**, 51 (1986).
[28] B. Li, G. Casati, J. Wang, and T. Prosen, Phys. Rev. Lett. **92**, 254301 (2004).
[29] H. B. Li, Q. M. Nie, and X. T. Xin, Chin. Phys. Lett. **26**, 074401 (2009).
[30] G. Benenti, G. Casati, and J. Wang, Phys. Rev. Lett. **110**, 070604 (2013).
[31] S. D. Chen, J. Wang, G. Casati, and G. Benenti, Phys. Rev. E **90**, 032134 (2014).
[32] J. Wang and G. Casati, Phys. Rev. Lett. **118**, 040601 (2017).
[33] R. X. Luo, G. Benenti, G. Casati, and J. Wang, Phys. Rev. Lett. **121**, 080602 (2018).
[34] J. L. Lebowitz and H. Spohn, J. Stat. Phys. **19**, 633 (1978); R. Tehver, F. Toigo, J. Koplik, and J. R. Banavar, Phys. Rev. E **57**, R17 (1998).
[35] G. Casati and T. Prosen, Phys. Rev. E **67**, 015203(R) (2003).
[36] J. P. Brantut, C. Grenier, J. Meineke, D. Stadler, S. Krinner, C. Kollath, T. Esslinger, and A. Georges, Science **342**, 713 (2013).